

## U–Pb Isotope and REE Composition of Zircon from the Pyroxene Crystalline Schists of the Irkut Terrane, Sharyzhalgai Uplift: Evidence for the Neoproterozoic Magmatic and Metamorphic Events

O. M. Turkina<sup>a</sup>, N. G. Berezhnaya<sup>b</sup>, L. N. Urmantseva<sup>a</sup>, I. P. Paderin<sup>b</sup>, and S. G. Skublov<sup>c</sup>

Presented by Academician V.V. Reverdatto February 15, 2009

Received February 25, 2009

DOI: 10.1134/S1028334X09090207

The Early Proterozoic granulite–gneissic complexes are typically characterized by a long evolutionary history, which involves formation of their protoliths and repeated metamorphism related mainly with collisional events. Zircons from high-grade metamorphic rocks usually consist of cores inherited from the protolith, and one or several mantles and rims that were formed during later metamorphism or partial melting. High-resolution methods of U–Pb dating make it possible to determine the age of cores and rims. However, knowledge of the trace-element composition of zircon is required in order to interpret correctly the obtained dates, because its zones that were grown or recrystallized at high-temperature metamorphism significantly differ in terms of REE distribution from their magmatic analogues [1–3]. This paper reports the results of study of zircons from high-grade basic rocks, i.e., pyroxene crystalline schists, which allowed us to determine the formation time of their magmatic protoliths and metamorphism, as well as to estimate the conditions of zircon formation.

The available data indicate that high-temperature metamorphism and granite formation in the Irkut block occurred in several stages. It was reliably established that Proterozoic metamorphism and related granite and charnockite formation spanned a time range of 1.88–1.85 Ga. These events were recorded in the formation of metamorphogenic zir-

cons, their rims, and baddeleyite in the metamorphic rocks, as well as magmatic zircons in the granitoids [4–7]. The lower age boundary of the Proterozoic stage of granulite metamorphism is constrained by the crystallization age of magmatic zircon from gabbro ( $2649 \pm 6$  Ma) metamorphosed under the granulite-facies metamorphism [7]. Vein granites cutting across the crystallization schistosity in metagabbro have an age of  $2562 \pm 20$  Ma. The Proterozoic granulite metamorphism and collisional granite formation of close age ( $\sim 2.6$  Ga and 2.53 Ga) were also established in the adjacent Kitoi granulite gneiss block [6].

The age of protoliths of metamorphic rocks and, correspondingly, the timing of early magmatic stages is the most controversial problem. The occurrence of at least two stages of metamorphic transformations and related granite formation of the Proterozoic (2.55–2.65 Ga) and Paleoproterozoic (1.85–1.87 Ga) ages points to the Archean age of the magmatic protoliths. Direct evidence for the presence of the Proterozoic rock associations is the results of U–Pb single zircon dating of pyroxene granulite from the southeastern termination of the Irkut block [6]. The cores in the zircon from the andesitic granulite have an age of  $3390 \pm 35$  Ma. According to our data, the manifestation of the Paleoproterozoic stage of crustal growth in the Irkut block is supported by values of the Nd model age ( $T_{Nd}(DM) = 2.9–3.6$  Ga) of the hypersthene–biotite orthogneisses.

The modern structure of the Irkut block is determined by the combination of the predominant granite and charnockite–gneiss domes and strongly deformed interdome zones. Detailed structural studies revealed two stages of folding and deformations [8]. The first stage was responsible for the formation of tightly compressed, narrow, mainly isoclinal folds preserved in the interdome zones, while the second stage produced charnockite (granite) gneiss domes. As was mentioned above, the domes were formed at the Paleoproterozoic stage of folding, metamorphism, and granite forma-

<sup>a</sup> Institute of Geology and Mineralogy, Siberian Branch, Russian Academy of Sciences, pr. Akademika Koptyuga 3, Novosibirsk, 630090 Russia  
e-mail: turkina@uiggm.nsc.ru

<sup>b</sup> Center of Isotopic Research, Karpinskii All-Russian Geological Research Institute, Srednii pr. 74, St. Petersburg, 199026 Russia

<sup>c</sup> Institute of Precambrian Geology and Geochronology, Russian Academy of Sciences, nab. Makarova 2, St. Petersburg, 199034 Russia

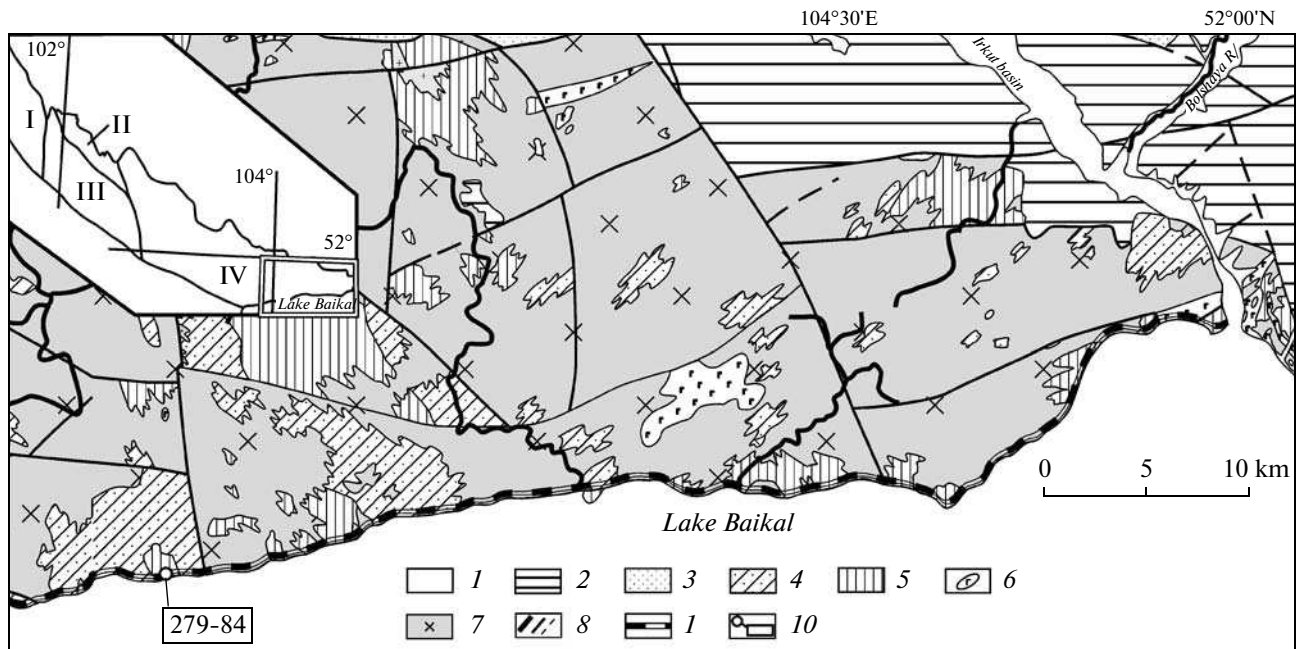


**Fig. 1.** Geological scheme of the southeastern Irkut block of the Sharyzhalgai Uplift. (1) Quaternary deposits; (2) Jurassic sediments; (3) undivided Sharyzhalgai Group; (4) garnet-biotite, biotite cordierite-bearing gneisses, calciphyres (Zhidoi Sequence), (5) hypersthene-bearing gneiss pyroxene crystalline schists (Shumikha Sequence), (6) Early Precambrian gabbroids; (7) Early Precambrian granitoids (undivided); (8) faults; (9) line of the CBRL; (10) locality of sample 279-84. Inset in the left corner shows the structure of the Sharyzhalgai Uplift. Blocks: (I) Bulun, (II) Onot, (III) Kitoi, (IV) Irkut.

tion. Isoclinally folded rocks in the interdome zones represent fragments of the metamorphic complex (Sharyzhalgai Group). In the intradome zone, the metamorphic rocks form relicts of visible size from tens of centimeters to a few tens of meters. The Sharyzhalgai metamorphic complex is made up of two-pyroxene and amphibole-pyroxene basic crystalline schists, amphibolites, biotite and amphibole-biotite hypersthene-bearing plagiogneisses, garnet-biotite, and aluminous cordierite and sillimanite-bearing gneisses. The hypersthene-bearing gneisses and two-pyroxene and amphibole-pyroxene basic crystalline schists alternate with each other or form individual fragments of the sequence. The crystalline schists are often observed as relicts among the granitoids of domal structures.

Crystalline schist (sample 279-84) was taken from relicts consisting of the crystalline schist and biotite ( $\pm$ hypersthene) gneisses among the granitoids (132.35 km of the Circum-Baikal Railway Line (CBRL)) (Fig. 1). The rock has a granoblastic texture and consists of plagioclase (~40–50%), clinopyroxene (50–60%), hornblende (~2–3%), orthopyroxene, and accessory minerals (zircon, magnetite, apatite).

Zircon was dated on a SHRIMP-II high-resolution ion microprobe at the Center of Isotopic Research of the Karpinskii All-Russia Geological Research Institute (St. Petersburg) using the technique described in [9]. The internal structure of the zircons was studied in cathodoluminescence (CL) as

well as by optical methods. Trace elements in zircon were analyzed by secondary ion mass spectrometry (ion probe) on a Cameca IMS-4F at the Institute of Microelectronics and Automatics of the Russian Academy of Sciences (Yaroslavl). The contents of major and trace elements in the rocks were determined by XRF and ICP-MS at the Analytical Center of the Institute of Geology and Mineralogy, Siberian Branch, Russian Academy of Sciences.

In terms of major elements, the crystal schists correspond to tholeiitic basalts subdivided into two types: low- and moderate-Ti. The first type is characterized by low contents of  $\text{TiO}_2$  (<1 wt %),  $\text{P}_2\text{O}_5$  (0.05–0.08%), Th (0.1–0.5 ppm), large ion lithophile elements (LILE), and LREE. Metabasalts show a flat rare-earth element pattern ( $\text{La}/\text{Sm}_n = 0.8–1.5$ ) and multi-element spectra with weakly expressed Nb anomalies ( $\text{Nb}/\text{Nb}^* = 0.7–1.7$ ) and Th depletion relative to La ( $\text{Th}/\text{La}_{pm} = 0.3–0.7$ ). Moderately Ti crystalline schists ( $\text{TiO}_2 = 1–3\%$ ;  $\text{P}_2\text{O}_5 = 0.1–0.26\%$ ) are enriched in Th, HFSE, and LREE. They are characterized by elevated ( $\text{La}/\text{Sm}_n$ ) (1.7–2.8), distinct negative Nb anomaly ( $\text{Nb}/\text{Nb}^* = 0.2–0.5$ ) in the spidergrams, and  $\text{Th}/\text{La}_{pm}$  (0.3–1.2) mainly below the corresponding value in the primitive mantle. The specifics of the trace element composition indicate that the two types of metabasalts were formed from different mantle sources and/or with variable contribution of crustal material. The dated sample is represented by moderate-Ti ( $\text{TiO}_2 = 1.59$  wt %) crystalline schist with a Zr content of 79 ppm.

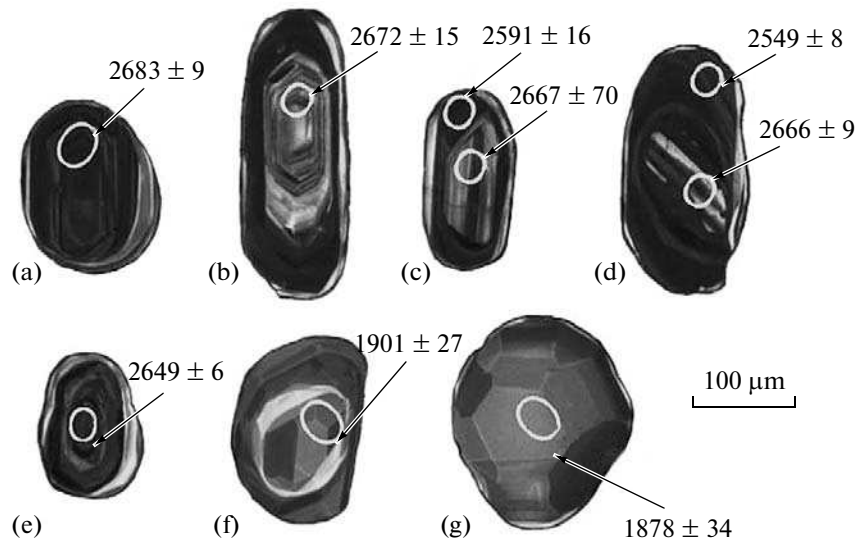


**Fig. 2.** Cathodoluminescent image of zircon from the pyroxene crystalline schist. (a–e) Prismatic zircon grains with zoned cores and metamorphic rims; (f, g) multifaceted grains of granulite zircon. The spots of dating and  $^{207}\text{Pb}/^{206}\text{Pb}$  age (Ma) are shown.

The sample contains zircon of two morphological types: predominant soccerball subequant “granulite” crystals of cherry and light pink color and less developed prismatic cherry crystals with smoothed edges and crystal tips. It is seen in CL-images that the prismatic crystals contain cores, dark rims, and thin light outer rims (Figs. 2a, 2b, 2c, 2d, 2e). Most of the cores preserve a prismatic shape. They are characterized by wide growth zones typical of the basic rocks (Figs. 2c, 2d); cores with thinner oscillatory zoning that are typical of felsic rocks are less common (Fig. 2b). This type of cores contains 194–350 ppm U, 169–236 ppm Th, and 0.5–1.2 Th/U ratio (table). CL-dark cores show weakly expressed zoning (Figs. 2a, 2e) and relative enrichment in Th (432–511 ppm) and, especially, U (685–1046 ppm), which can result from their metasomatic reworking. CL-dark structureless shells are sharply enriched in U (1008–1910 ppm), depleted in Th (27–34 ppm), and have an extremely low Th/U ratio (0.03). Weak zoning or its absence is typical of metamorphic zircons [10]. Soccerball crystals of cherry color are characterized by dull luminescence, while pink crystals show bright luminescence and sectorial zoning. The sectorial zoned multifaceted crystals of zircons are considered to be formed by high-temperature subsolidus growth [11]. The zircon of this type is depleted in Th (22–56 ppm) and U (125–248 ppm) at a lower Th/U ratio (0.17–0.25).

The distinguished generations of the zircon distinctly differ in trace element composition. Prismatic cores with both coarse and thinner zoning have similar REE patterns with steep HREE enrichment  $[(\text{Lu}/\text{Gd})_n = 12\text{--}30$  (Fig. 3)] typical of zircons from magmatic rocks, including zircons from gabbro  $[(\text{Lu}/\text{Gd})_n = 16\text{--}44]$ , and diorites  $[(\text{Lu}/\text{Gd})_n = 27]$  [2]. The LREE and

MREE patterns show wider variations. Two cores have higher Ce contents and a sharply expressed positive Ce anomaly ( $\text{Ce}/\text{Ce}^* = 67\text{--}187$ ), they are relatively rich in Sm and Eu that defines high value of  $(\text{Sm}/\text{La})_n$  (123–144), as well as a weakly expressed Eu anomaly ( $\text{Eu}/\text{Eu}^* = 0.5\text{--}0.6$ ). Two other cores with thin oscillatory and coarse zoning in terms of Ce ( $\text{Ce}/\text{Ce}^* = 19\text{--}40$ ) and Eu ( $\text{Eu}/\text{Eu}^* = 0.12\text{--}0.3$ ) anomalies are close to zircons from the gabbro and diorites ( $\text{Ce}/\text{Ce}^* = 20\text{--}39$ ,  $\text{Eu}/\text{Eu}^* = 0.2$ ). In general, in terms of characteristic ratios, the studied cores fall in the interval of magmatic rocks of a wide  $\text{SiO}_2$  range:  $(\text{Sm}/\text{La})_n = 57\text{--}547$  and  $(\text{Lu}/\text{Gd})_n = 16\text{--}74$  [2], which indicates their magmatic origin. Noted variations in LREE and Eu behavior are not correlated with the type of zoning and give no grounds to suggest a xenogenic nature of the some studied cores. The wide dark rims of the prismatic crystals with a low Th/U ratio (0.03) typical of metamorphic zircons as compared to the magmatic zircons are distinctly depleted in Y, P, REE, have a weakly expressed positive Ce anomaly ( $\text{Ce}/\text{Ce}^* = 5\text{--}7$ ), and a flatter HREE distribution  $[(\text{Lu}/\text{Gd})_n = 3.7\text{--}4.2]$ . Such low  $(\text{Lu}/\text{Gd})_n$  ratios are typical of zircons from granulites and eclogites [1, 3]. LREE and HREE depletion was established in the granulite zircons that crystallized in the presence of monazite and garnet, respectively [1]. The tendency to REE depletion is also preserved for multifaceted zircon crystals, which are characterized by a flat HREE pattern  $[(\text{Lu}/\text{Gd})_n = 6\text{--}11]$ , moderate positive Ce anomaly ( $\text{Ce}/\text{Ce}^* = 9\text{--}24$ ), and, in addition, a weakly expressed negative Eu anomaly ( $\text{Eu}/\text{Eu}^* = 0.7\text{--}0.8$ ).

Five cores (1.1, 2.1, 4.1, 5.1, 10.1) define a discordia with the upper intercept at  $2662 \pm 16$  Ma (MSWD = 2.4) (Fig. 4). This value within the error corresponds to the concordant age of  $2683 \pm 9$  Ma obtained for the

## U–Pb isotope data and age of zircons from the pyroxene crystalline schist of the Irkut block

Spot	$^{206}\text{Pb}_c$ , %	U, ppm	Th, ppm	$^{232}\text{Th}/^{238}\text{U}$	$^{206}\text{Pb}^*$ , ppm	Age, Ma	
						$^{206}\text{Pb}/^{238}\text{U}$	$^{207}\text{Pb}/^{206}\text{Pb}$
279-84.1.1c	0.09	685	432	0.65	319	2794 ± 49	2649 ± 6
279-84.2.1c	0.13	194	236	1.26	90.6	2800 ± 53	2667 ± 12
279-84.2.2r	0.02	716	40	0.06	337	2814 ± 50	2591 ± 16
279-84.3.1c	0.36	214	35	0.17	100	2804 ± 53	2618 ± 30
279-84.4.1c	0.03	317	169	0.55	146	2772 ± 51	2672 ± 15
279-84.5.1c	0.01	350	169	0.50	148	2579 ± 48	2666 ± 9
279-84.5.2r	0.06	666	26	0.04	279	2558 ± 52	2549 ± 8
279-84.6.1r	0.25	363	162	0.46	126	2179 ± 41	2274 ± 18
279-84.7.1g	0.14	161	50	0.32	50	1983 ± 41	1901 ± 27
279-84.8.1g	0.18	117	39	0.34	35.6	1948 ± 43	1878 ± 34
279-84.9.1r	0.37	55	14	0.27	22.6	2518 ± 62	2336 ± 47
279-84.10.1c	0.01	1046	511	0.51	465	2688 ± 47	2683 ± 9
279-84.11.1g	1.08	87	21	0.25	28.8	2081 ± 48	1812 ± 53

Spot	<i>D</i> , %	$^{238}\text{U}/^{206}\text{Pb}^*$	±%	$^{207}\text{Pb}^*/^{206}\text{Pb}^*$	±%	$^{207}\text{Pb}^*/^{235}\text{U}$	±%	$^{206}\text{Pb}^*/^{238}\text{U}$	±%	Err. corr.
279-84.1.1c	−5	1.843	2.2	0.17956	0.39	13.43	2.2	0.542	2.2	0.984
279-84.2.1c	−5	1.839	2.3	0.1815	0.73	13.61	2.5	0.544	2.3	0.955
279-84.2.2r	−8	1.827	2.2	0.1734	0.95	13.08	2.4	0.547	2.2	0.918
279-84.3.1c	−7	1.835	2.3	0.1763	1.8	13.24	3	0.545	2.3	0.787
279-84.4.1c	−4	1.861	2.2	0.1821	0.92	13.49	2.4	0.537	2.2	0.925
279-84.5.1c	3	2.033	2.2	0.18142	0.52	12.31	2.3	0.492	2.2	0.974
279-84.5.2r	0	2.053	2.5	0.16917	0.46	11.36	2.5	0.487	2.5	0.983
279-84.6.1r	4	2.487	2.2	0.1438	1	7.97	2.5	0.4021	2.2	0.906
279-84.7.1g	−4	2.776	2.4	0.1164	1.5	5.78	2.9	0.3602	2.4	0.846
279-84.8.1g	−4	2.834	2.5	0.1149	1.9	5.59	3.2	0.3528	2.5	0.806
279-84.9.1r	−7	2.093	3	0.1491	2.7	9.83	4.1	0.478	3	0.738
279-84.10.1c	0	1.933	2.1	0.1833	0.56	13.08	2.2	0.517	2.1	0.967
279-84.11.1g	−13	2.624	2.7	0.1108	2.9	5.82	4	0.381	2.7	0.679

Note: Abbreviations: (c) core, (r) rim, (g) multifaceted crystal. Errors are given at 1 $\sigma$  level.  $\text{Pb}_c$  and  $\text{Pb}^*$  are common and radiogenic lead, respectively. The error in standard calibration was no more than 0.88%. *D* is discordance; negative values are reverse discordant ages. Err. corr. is correlation coefficient of the  $^{207}\text{Pb}^*/^{235}\text{U}$  and  $^{206}\text{Pb}^*/^{238}\text{U}$  ratios.

CL-dark core in zircons with smoothed peaks and edges (Fig. 2a). Taking into account the presence of zoning in the prismatic cores, their Th/U ratios (0.48–1.2), as well as the REE distribution typical of magmatic zircons, the established age should be considered as the crystallization age of the magmatic protolith of the crystalline schists. Dark rims (2.2, 5.2) and one of the cores (3.1) are characterized by age values within the range of 2549–2618 Ma. Their low Th/U ratio (0.04–0.16) and HREE depletion relative to cores suggest that growth of the rims and recrystallization of the cores were related to the early metamorphic stage, whose age was estimated from the concordant point to be 2549 ± 8 Ma. The age of pink multifaceted crystals of zircon with sectorial zoning

accounts for 1880 ± 39 Ma. Their growth was obviously related to the Paleoproterozoic granulite metamorphism. It should be noted that zircons of the Paleoproterozoic age differ only in the moderately lowered Th/U ratio (0.31–0.33), whereas the contents of U (55–117 ppm) and especially Th (14–39 ppm) in the zircons are significantly lower than those in the magmatic cores. Close Th/U ratios (0.26–0.45) were established also for two subsequent crystals with intermediate age values of 2274 and 2336 Ma, which could be interpreted as the result of incomplete reworking of the Archean zircons during Paleoproterozoic metamorphism.

The specifics of REE distribution in the zircons of three age generations provide insight into the condi-

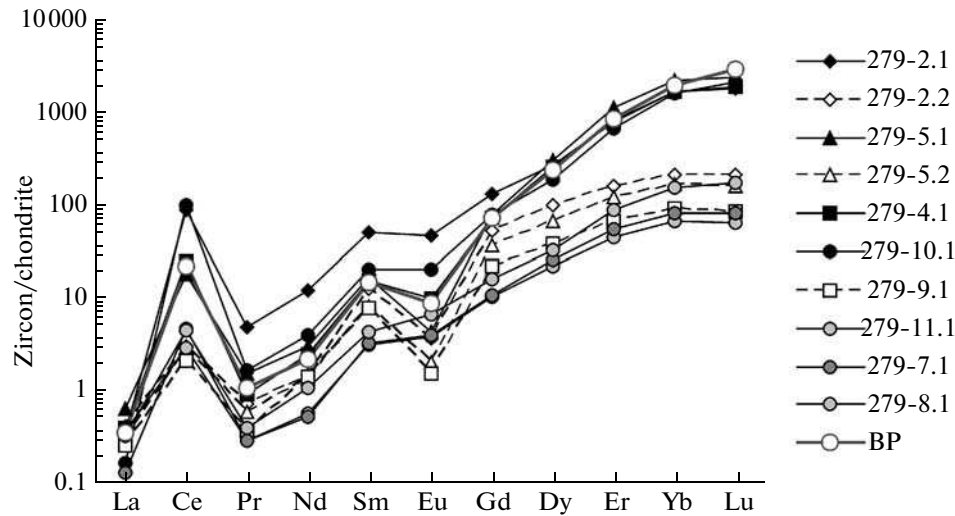


**Fig. 3.** REE distribution in zircons (sample 279-84). Spots: 2.1, 5.1, 4.1, 10.1 are cores; 2.2, 5.2, 9.1 are rims, 11.1, 7.1, 8.1 are multifaceted crystals (spot numbers correspond to those in the table). (BP) is zircon from gabbro [2].

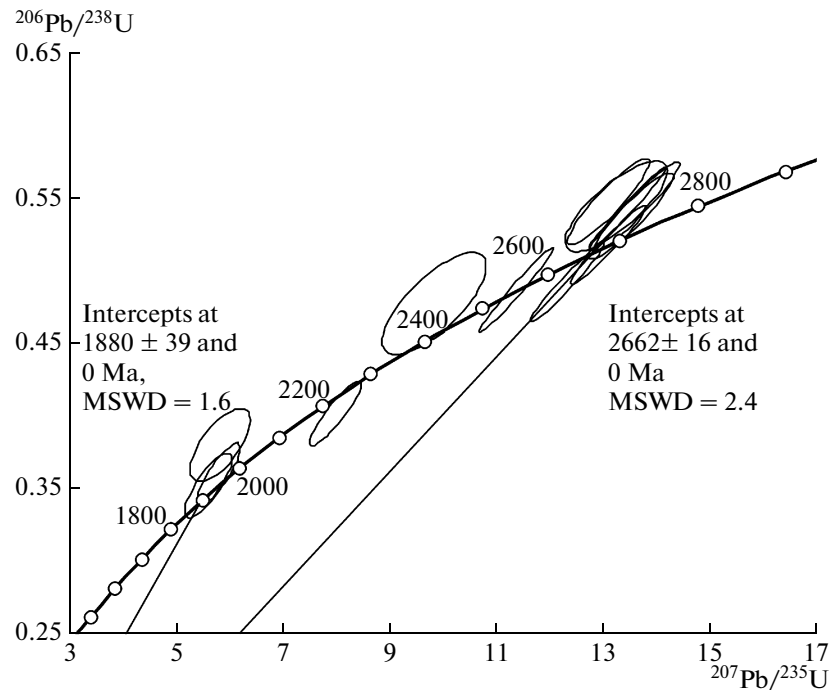


**Fig. 4.** Concordia diagram for zircons from the crystalline schist (Sample 279-84).

tions of their formation. The REE patterns for zircon cores with rhythmic zoning suggest their magmatic origin. A sharp decrease in HREE with decreasing  $(\text{Lu}/\text{Gd})_n$  and less expressed flattening of LREE spectra found in unzoned rims is indicative of zircons that are formed under high-grade metamorphism, with concurrent growth of garnet and monazite accumulating, respectively, HREE and LREE [1, 3]. However, the crystalline schists do not contain these minerals. A decrease in the contents of trace elements that are not

the main structural components of zircon could be result of its recrystallization during metamorphism [12]. Since, as is known, the possibility of isomorphous incorporation of admixtures in a mineral structure decreases with decreasing temperature, the observed REE depletion in rims is probably related to the lower temperature during the Archean metamorphism as compared to conditions of crystallization of zircon cores from the melts of basic composition. The exception is U, high concentrations of which in the

rims are likely caused by the presence of metamorphic fluid with a high U content owing to the extraction of the latter from the structure of the rock-forming minerals. A trend of REE depletion was also established in the Paleoproterozoic “granulite” zircons. The decrease in the negative Eu anomaly in these zircons is supposedly related to their earlier formation relative to plagioclase. This type of zircon has extremely low contents of not only Th, but also U. The U depletion was possibly caused by its removal with the fluid phase, because during granulite metamorphism fluid acquires an essentially hydrocarbonic composition, which facilitates migration of U in the form of uranyl–carbonate complexes. Thus, the growth of rims and soccerball zircon crystals is obviously related to the high-temperature metamorphism, while REE depletion observed in the metamorphogenic zircons was presumably caused by recrystallization rather than concurrent growth of garnet and monazite.

Based on the internal structure and rare-element and isotope composition, three zircon generations of different ages were distinguished in the crystalline schists: magmatic cores, metamorphic rims, and multifaceted “granulite” crystals. The age of the magmatic protolith of the crystalline schists established from zircon cores accounts for ~2.66 Ga. The occurrence of basic volcanism correlated with the global peak (2.8–2.6 Ga) of crustal growth in the Late Archean, which manifested itself on all the continents (see [13]). The formation of rims and multifaceted zircon crystals marks two stages of high-temperature metamorphism (~2.55 and ~1.88 Ga). The metamorphism of the crystalline schists occurred simultaneously with epochs of accretionary–collisional processes, which, in turn, correlate with formation of the Neoproterozoic and Paleoproterozoic supercontinents.

## ACKNOWLEDGMENTS

This work was supported by the Russian Foundation for Basic Research (project no. 09-05-00382).

## REFERENCES

1. D. Rubatto, *Chem. Geol.* **184**, 123–138 (2002).
2. P. W. O. Hoskin and U. Schaltegger, *Rev. Mineral. Geochem.* **53**, 27–62 (2003).
3. A. A. Fedotova, E. V. Bibikova, and S. G. Simakin, *Geokhimiya*, No. 9, 980–997 (2008) [*Geochem. Int.* **46**, 912 (2008)].
4. E. V. Bibikova, *Uranium–Lead Geochronology of the Early Evolutionary Stages of Ancient Shields* (Nauka, Moscow, 1989) [in Russian].
5. M. Aftalion, E. V. Bibikova, D. R. Bowes, et al., *J. Geol.* **99**, 851–861 (1991).
6. U. Poller, D. Gladkochub, T. Donskaya, et al., *Precambrian Res.* **136**, 353–368 (2005).
7. E. B. Sal’nikova, A. B. Kotov, V. I. Levitskii, et al., *Stratigr. Geol. Korrelyatsiya* **15** (4), 3–19 (2007) [*Stratigr. Geol. Correlation* **15**, 343 (2007)].
8. A. M. Hoggood and D. R. Bowes, *Tectonophysics* **174**, 279–299 (1990).
9. O. M. Turkina, N. G. Berezhnaya, A. N. Larionov, et al., *Geol. Geofiz.* **50** (1), 21 (2009).
10. F. Corfu, J. M. Hanchar, P. W. O. Hoskin, et al., *Rev. Mineral. Geochem.* **53**, 469–500 (2003).
11. U. Schaltegger, C. M. Fanning, D. Gunther, et al., *Contrib. Mineral. Petrol.* **134**, 186–201 (1999).
12. P. W. O. Hoskin and L. P. Black, *J. Metamorph. Geol.* **18**, 423–439 (2000).
13. K. Condie, *Earth Planet. Sci. Lett.* **163**, 97–108 (1998).